Supplemental Data

Supplemental Tables

Table S1. Results of crosses to generate *Mdm2*$^{-/-}$ mice with the *p53*^{neo} allele

Cross: *p53*$^{neo/neo}$ *Mdm2*$^{+/-}$ × *p53*$^{-/-}$ *Mdm2*$^{-/-}$

	Expected Genotypes	
Age (weeks)	***p53*$^{neo/-}$ *Mdm2*$^{+/-}$**	***p53*$^{neo/-}$ *Mdm2*$^{-/-}$**
0	12*	10
1	12	10
2	12	3
3	12	0

Cross: *p53*$^{neo/neo}$ *Mdm2*$^{+/-}$ × *p53*$^{R172H/R172H}$ *Mdm2*$^{-/-}$

	Expected Genotypes	
Age (weeks)	***p53*$^{neo/R172H}$ *Mdm2*$^{+/-}$**	***p53*$^{neo/R172H}$ *Mdm2*$^{-/-}$**
5	8	8

* number of pups obtained from cross

Table S2. Summary of tumor response in *p53$^{neo/-}$*, *p53$^{neo/R172H}$*, *p53$^{neo/-}$ Cre-ER^{TM}*, and *p53$^{neo/R172H}$ Cre-ER^{TM}* mice after tamoxifen treatment

Tumor #	Mouse #	Genotype	Tumor Type	Tumor Volume(cm^3)		Change in Tumor Volume (%)	Survival (days)
				V0	V1		
L1	NNE173	*p53$^{neo/-}$*	T-lymphoma	0.127	0.229	74.3	7
L2	M2-274	*p53$^{neo/-}$*	T-lymphoma	0.242	1.063	339.0	14
L3	NNE109	*p53$^{neo/-}$*	Lymphoma	0.619	3.020	387.9	10
L4	NNE117	*p53$^{neo/-}$ ER*	Lymphoma	0.264	0.013	-95.1	28*
L5	NNE49	*p53$^{neo/-}$ ER*	T-lymphoma	0.562	0.138	-75.4	16#
L6	NNE164	*p53$^{neo/-}$ ER*	Lymphoma, lymph node	0.134	0.053	-60.5	28*#
L7	NNE46	*p53$^{neo/-}$ ER*	Lymphoma	0.656	0.411	-37.4	24
L8	NHE182	*p53$^{neo/H}$*	T-lymphoma	0.117	0.309	164.1	7
L9	NHE167	*p53$^{neo/H}$*	T-lymphoma	0.499	1.443	189.2	8
L10	ER266	*p53$^{neo/H}$*	Lymphoma	0.326	1.023	213.8	6
L11	NHE179	*p53$^{neo/H}$*	T-lymphoma	0.09	0.771	756.7	7
L12	NHE191	*p53$^{neo/H}$*	Lymphoma	0.176	2.001	1036.4	9
L13	NHE166	*p53$^{neo/H}$ ER*	T-lymphoma	1.005	0.99	-1.5	25
L14	NHE131	*p53$^{neo/H}$ ER*	T-lymphoma	0.044	0.044	0.000	23
L15	NHE160	*p53$^{neo/H}$ ER*	T-lymphoma	0.087	0.101	16.1	28*
L16	NHE141	*p53$^{neo/H}$ ER*	Lymphoma, lymph node	0.138	0.181	31.2	28*
L17	NHE139	*p53$^{neo/H}$ ER*	Lymphoma	0.103	0.149	44.7	28*
S1	NNE153	*p53$^{neo/-}$*	Osteosarcoma	0.706	1.181	67.3	15
S2	NE199	*p53$^{neo/-}$*	Angiosarcoma	0.634	1.179	86.0	12
S3	NNE31	*p53$^{neo/-}$*	Angiosarcoma	0.189	0.419	118.0	10
S4	NE220	*p53$^{neo/-}$*	Angiosarcoma	0.334	0.845	153.0	14
S5	NNE113	*p53$^{neo/-}$*	Angiosarcoma	0.333	1.076	223.1	21
S6	NNE158	*p53$^{neo/-}$ ER*	Angiosarcoma	0.184	0.002	-98.9	28*
S7	NNE47	*p53$^{neo/-}$ ER*	Giant-cell sarcoma	0.058	0.025	-56.9	28*
S8	M2-236	*p53$^{neo/-}$ ER*	Angiosarcoma	0.96	0.603	-37.2	28*
S9	M2-234	*p53$^{neo/-}$ ER*	Angiosarcoma	0.257	0.21	-18.3	28*
S10	ER270	*p53$^{neo/H}$*	Angiosarcoma	0.181	0.444	145.3	8
S11	NHE137	*p53$^{neo/H}$*	Angiosarcoma	0.657	2.666	305.8	11
S12	NHE147	*p53$^{neo/H}$*	Angiosarcoma	0.312	2.251	621.5	14
S13	NHE113	*p53$^{neo/H}$ ER*	Angiosarcoma	0.123	0.132	7.3	20
S14	NHE126	*p53$^{neo/H}$ ER*	Angiosarcoma	0.411	0.454	10.5	28*#
S15	NHE111	*p53$^{neo/H}$ ER*	Angiosarcoma	0.055	0.067	21.8	28*

* endpoint of the experiment

mouse had second tumor upon autopsy which was not analyzed by MRI

Supplemental Figures

Figure S1

Figure S1. p53 Levels in *p53*$^{+/-}$ and *p53* Wild-Type MEFs

Western blot analysis of p53 expression in doxorubicin-treated MEFs of *p53*$^{-/-}$ (–/–), *p53*$^{+/-}$ (+/–), and *p53* wild type (+/+). Levels of p53 were normalized to actin.

Figure S2

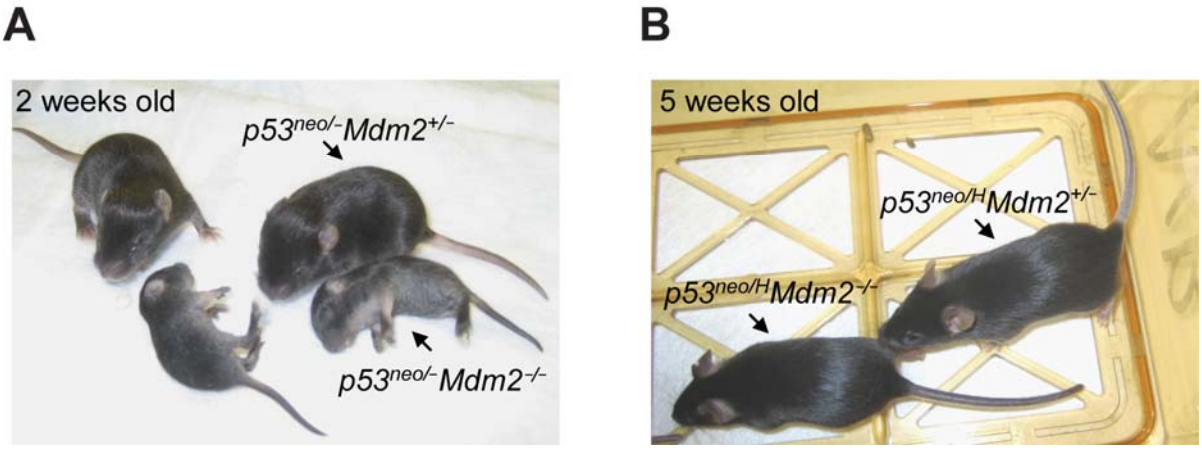

Figure S2. *p53*$^{neo/-}$ and *p53*$^{neo/R172H}$ Rescued Embryonic Lethality of *Mdm2*-Null Mice

(A) *p53*$^{neo/-}$ partially rescues the *Mdm2*-null phenotype. The picture shows different body sizes between *p53*$^{neo/-}$ *Mdm2*$^{-/-}$ and *p53*$^{neo/-}$ *Mdm2*$^{+/-}$ littermates at 2 weeks of age. (B) *p53*$^{neo/R172H}$ (*neo/H*) completely rescues *Mdm2*-null phenotype. *p53*$^{neo/R172H}$ *Mdm2*$^{-/-}$ mice developed normally, as shown in the picture of two 5 week old *p53*$^{neo/R172H}$ *Mdm2*$^{-/-}$ and *p53*$^{neo/R172H}$ *Mdm2*$^{+/-}$ littermates.

Figure S3

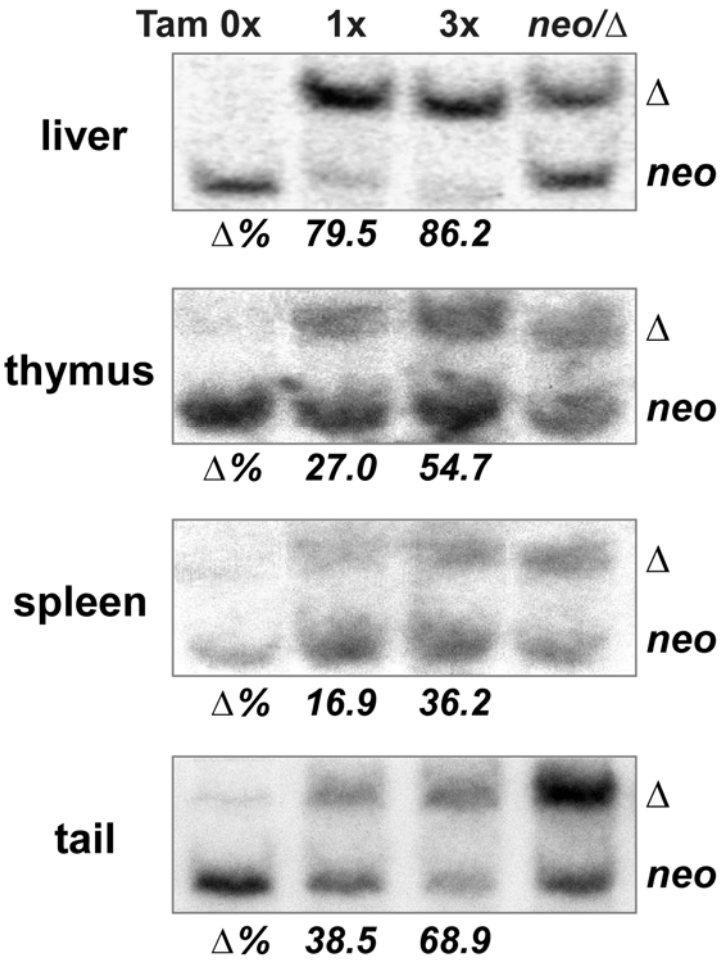

Figure S3. *p53*^{neo} Recombination in Tamoxifen-Treated *p53*$^{neo/-}$ *Cre-ER*^{TM} Mice

Genomic DNAs from vehicle- or tamoxifen (Tam)-treated *p53*$^{neo/-}$ *Cre-ER*^{TM} mouse tissues (0x, vehicle treatment; 1x, tamoxifen treatment once; 3x, three tamoxifen treatments) were subject to Southern blot analysis using a probe that bound to both the *p53*^{neo} (neo) and *p53*$^{\Delta neo}$ (Δ) alleles. The numbers under lanes indicate the % recombination of the p53^{neo} to *p53*$^{\Delta neo}$ (Δ%). Genomic DNAs from tissues of *p53*$^{neo/\Delta neo}$ mice were loaded as controls.

Figure S4

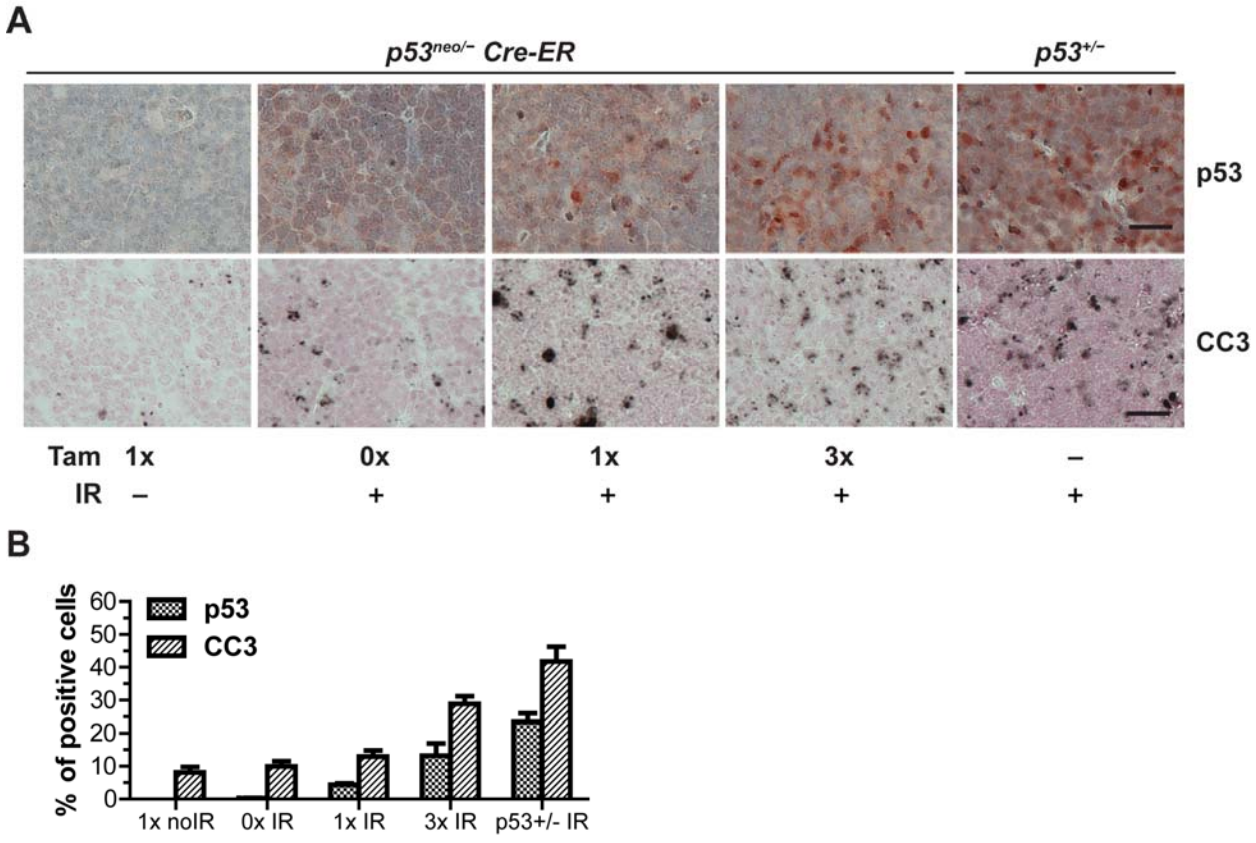

Figure S4. In Vivo p53 Restoration in Thymus

(A) Immunohistochemistry of p53 and cleaved caspase 3 (CC3) in the thymus of vehicle- or tamoxifen (Tam)-treated *p53*$^{neo/–}$ *Cre-ER*^{TM} mice (0x, vehicle treatment; 1x, tamoxifen treatment once; 3x, tamoxifen treatment three times) exposed to 6 Gy γ-radiation (IR). Tissues were collected 5 hours after IR. The irradiated *p53*$^{+/–}$ mice were used as a positive control, and tamoxifen-treated *p53*$^{neo/–}$ *Cre-ER*^{TM} mice without γ-radiation (no IR) as a negative control. Scale bar, 20 μm. (B) Percentages of cells staining positive for p53 and CC3 in A.

Figure S5

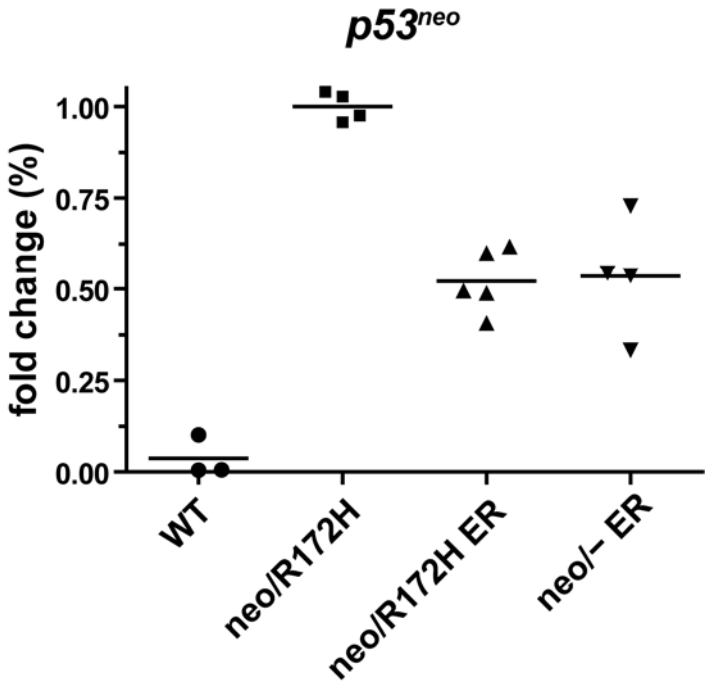

Figure S5. *p53*^{neo} Recombination in *p53*$^{neo/–}$ *Cre-ER*^{TM} and *p53*$^{neo/R172H}$ *Cre-ER*^{TM} Lymphomas after Tamoxifen Treatment.

The levels of the *p53*^{neo} allele remaining in tumor DNA samples were analyzed by quantitative real-time PCR. Samples were analyzed from wild-type (*WT*) and *p53*$^{neo/R172H}$ (*neo/R172H*) mouse tissues, and from *p53*$^{neo/R172H}$ *Cre-ER*^{TM} (*neo/R172H Cre-ER*) and *p53*$^{neo/–}$ *Cre-ER*^{TM} (*neo/– Cre-ER*) tumor tissues.

Figure S6

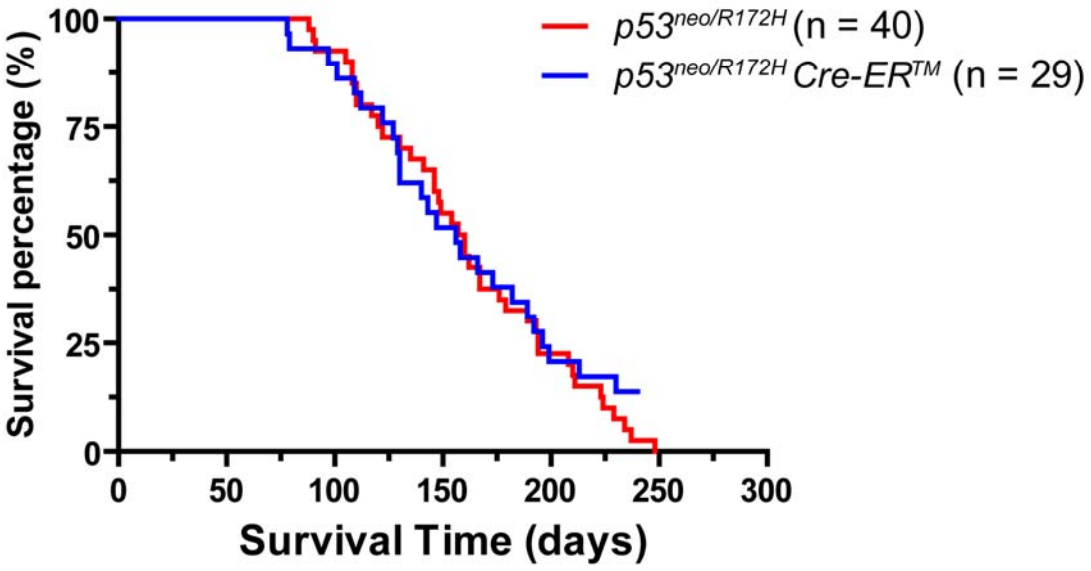

Figure S6. Survival Curves of *p53*$^{neo/R172H}$ and *p53*$^{neo/R172H}$ *Cre-ER*^{TM} Mice.

Figure S7

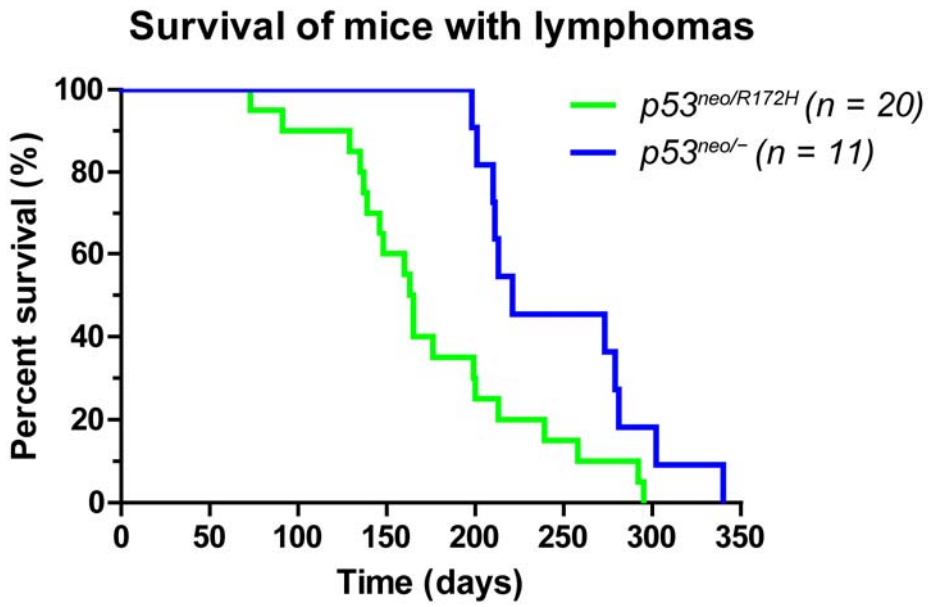

Figure S7. Survival Curves of *p53*$^{neo/-}$ and *p53*$^{neo/R172H}$ Mice with Lymphomas.

Figure S8

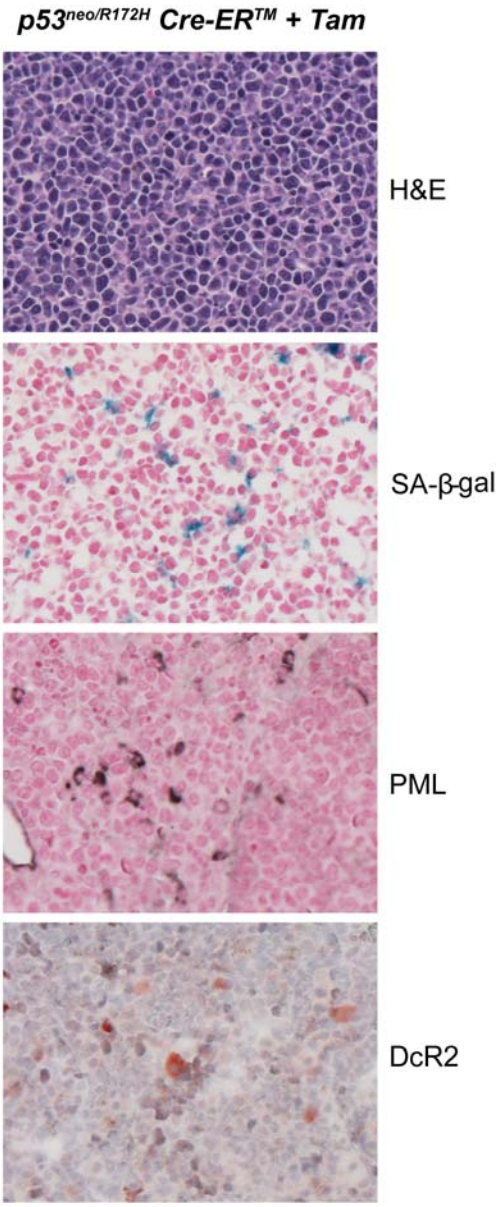

Figure S8. p53 Restoration Induced Senescence in *p53*$^{neo/R172H}$ *Cre-ER*^{TM} Lymphomas

A representative lymphoma collected from a *p53*$^{neo/R172H}$ *Cre-ER*^{TM} mouse 3 days after tamoxifen (Tam) treatment, was subjected to hematoxylin and eosin (H&E) staining, SA-β-gal assay, and immunohistochemical staining for senescence markers PML and DcR2.

Figure S9

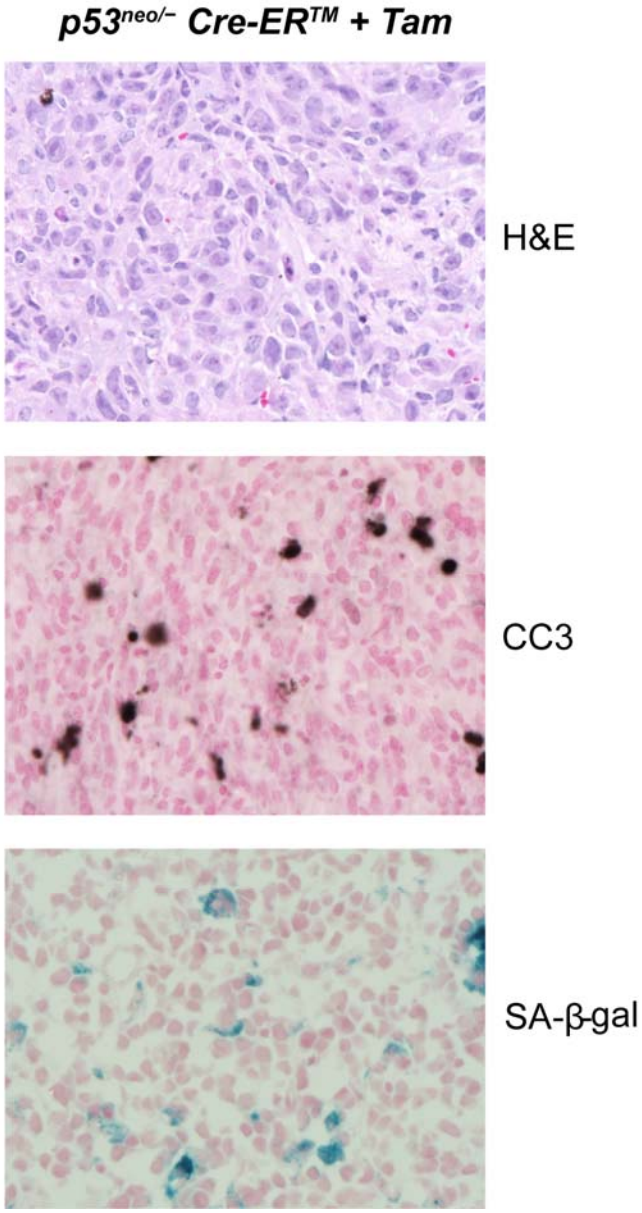

Figure S9. p53 Restoration Induced both Apoptosis and Senescence in a *p53*$^{neo/–}$ *Cre-ER*^{TM} Giant-Cell Sarcoma

The tamoxifen (Tam)-treated sarcoma was subjected to hematoxylin and eosin (H&E) staining, immunohistochemical staining for cleaved caspase 3 (CC3), and senescence-associated β-galactosidase (SA-β-gal) assay.

Figure S10

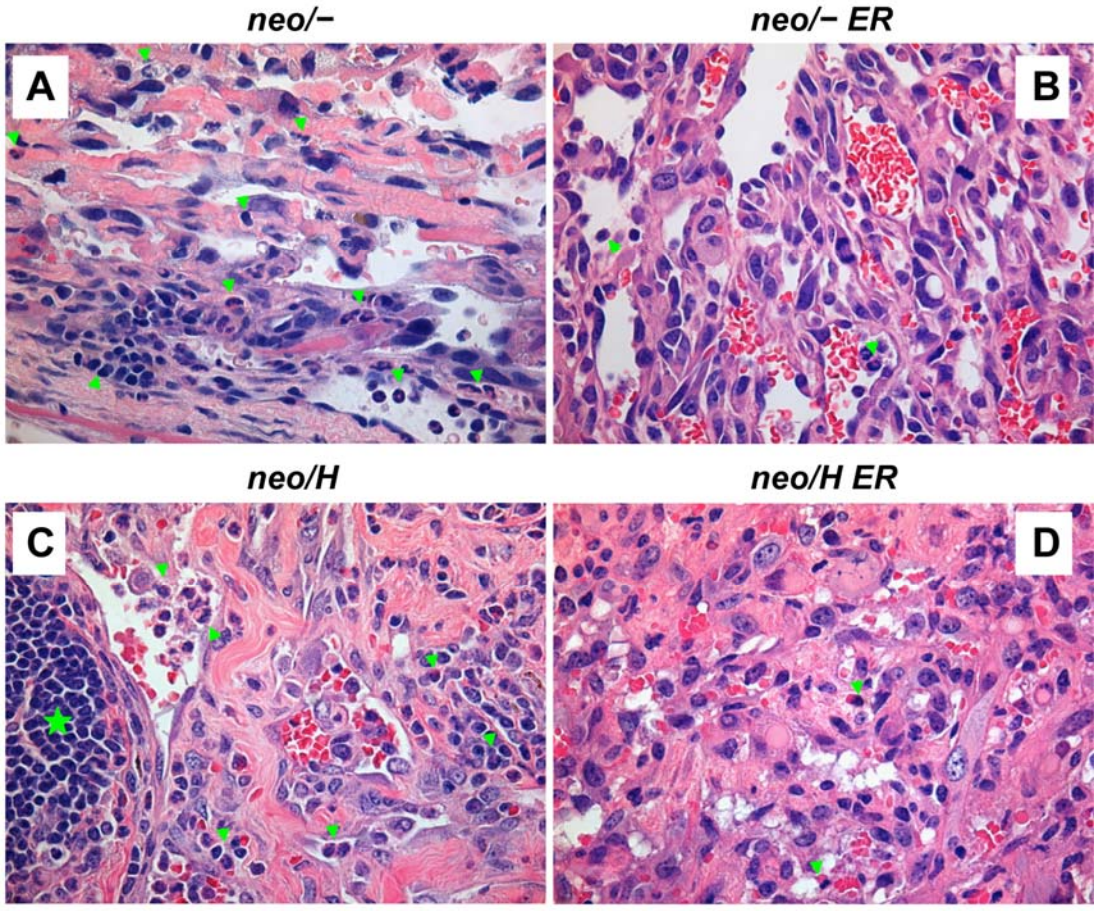
neo/−
neo/− ER
A
B
neo/H
neo/H ER
C
D

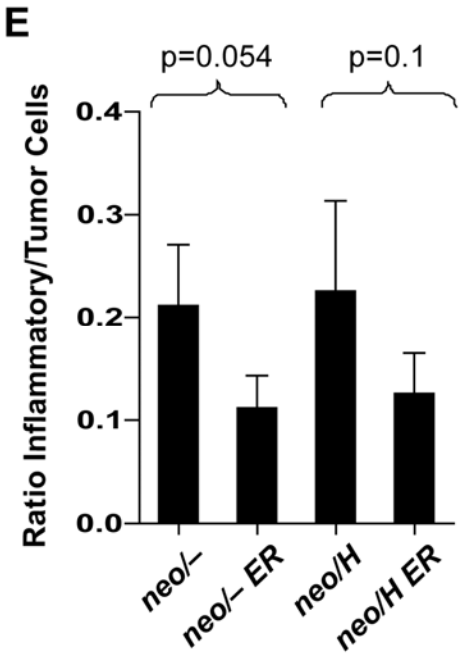
E
p=0.054
p=0.1
Ratio Inflammatory/Tumor Cells
0.4
0.3
0.2
0.1
0.0
neo/−
neo/− ER
neo/H
neo/H ER

Figure S10. Immune Infiltration in Tumors following p53 Reactivation.

The inflammatory cell burden in angiosarcomas of different genotypes was determined by counting the number of polymorphonuclear cells and lymphocytes in areas devoid of focal inflammatory aggregates. $p53^{neo/-}$ (*neo/–*, A) and $p53^{neo/R172H}$ (*neo/H*, C) tumors harbored a higher number of interstitial inflammatory cells compared to their respective $p53^{neo/-}$ *Cre-ER*^{TM} (*neo/– ER*, B) and $p53^{neo/R172H}$ *Cre-ER*^{TM} (*neo/H ER*, D) tumor counterparts (median ratio of inflammatory cells to tumor cells in $p53^{neo/-}$ vs $p53^{neo/-}$ *Cre-ER*^{TM}, 0.18 vs 0.11, p=0.054; $p53^{neo/R172H}$ vs $p53^{neo/R172H}$ *Cre-ER*^{TM}, 0.15 vs 0.16, p=0.1, E). Histological analysis revealed that $p53^{neo/-}$ and $p53^{neo/R172H}$ tumors had occasional focal inflammatory aggregates (green star) which were rare in $p53^{neo/-}$ *Cre-ER*^{TM} and $p53^{neo/R172H}$ *Cre-ER*^{TM} tumors. Arrows denote peritumoral inflammatory polymorphonuclear cells and lymphocytes. At least 300 cells were counted from three random high magnification fields per tumor. The mean and SEM for each genotype were calculated from at least three tumors per genotype.

Figure S11

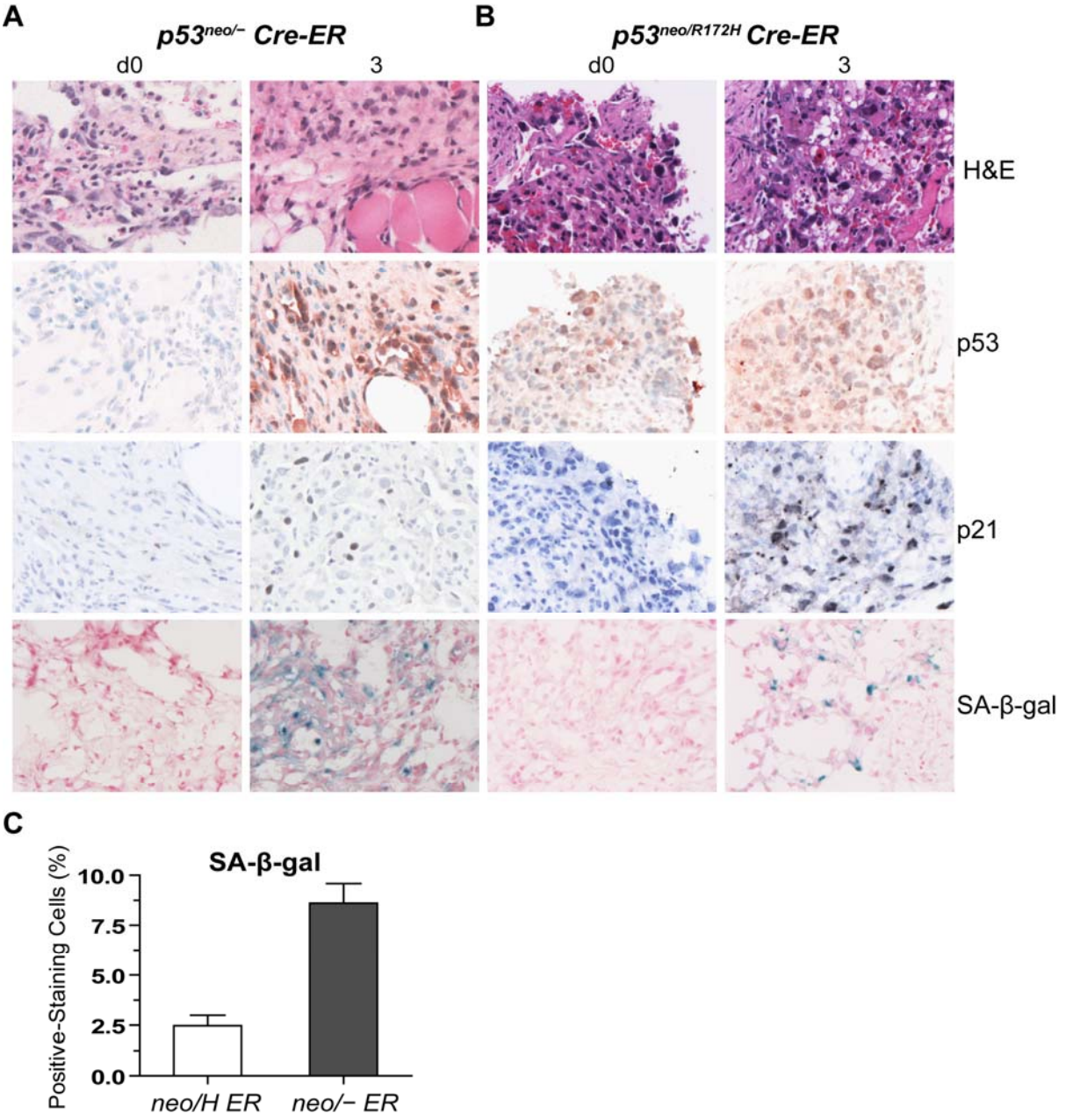

Figure S11. p53 Activation in Angiosarcomas after Tamoxifen Treatment

Tumor specimens harvested from *p53*$^{neo/–}$ *Cre-ER*^{TM} and *p53*$^{neo/R172H}$ *Cre-ER*^{TM} mice, before (d0) and 3 days after tamoxifen treatment (d3) were subjected to hematoxylin and eosin (H&E) staining, immunohistochemical staining for p53 and p21, and SA-β-gal assay. (A) Images of biopsies from an angiosarcoma in a *p53*$^{neo/–}$ *Cre-ER*^{TM} *(neo/– ER)* mouse (d0 and 3). (B) Images of biopsies from an angiosarcoma in a *p53*$^{neo/R172H}$ *Cre-ER*^{TM} (*neo/H ER*) mouse (d0 and 3). (C) Percentage of β-gal-positive-staining cells at d3 of A & B.

Figure S12

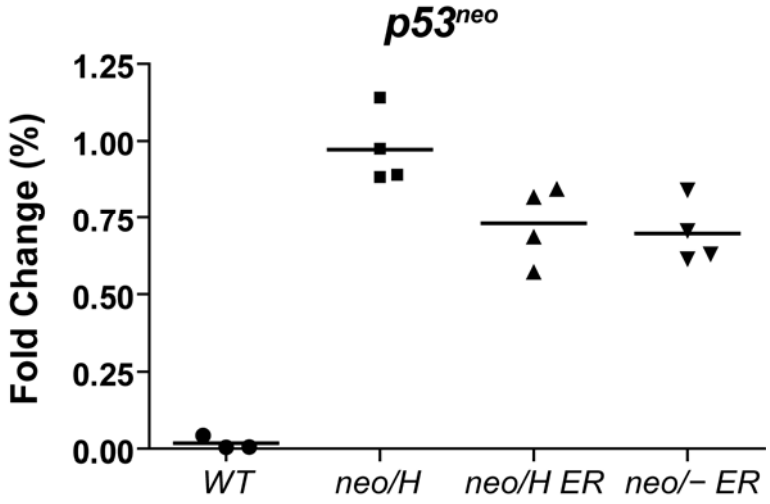

Figure S12. *p53*^{neo} Recombination in *p53*$^{neo/-}$ *Cre-ER*^{TM} and *p53*$^{neo/R172H}$ *Cre-ER*^{TM} Angiosarcomas after Tamoxifen Treatment

The levels of the *p53*^{neo} allele remaining in tumor DNA samples were analyzed by quantitative real-time PCR. Samples were analyzed from wild-type (*WT*) and *p53*$^{neo/R172H}$ (*neo/H*) mouse tissues, and from *p53*$^{neo/R172H}$ *Cre-ER*^{TM} (*neo/H ER*) and *p53*$^{neo/-}$ *Cre-ER*^{TM} (*neo/− ER*) tumor tissues.

Figure S13

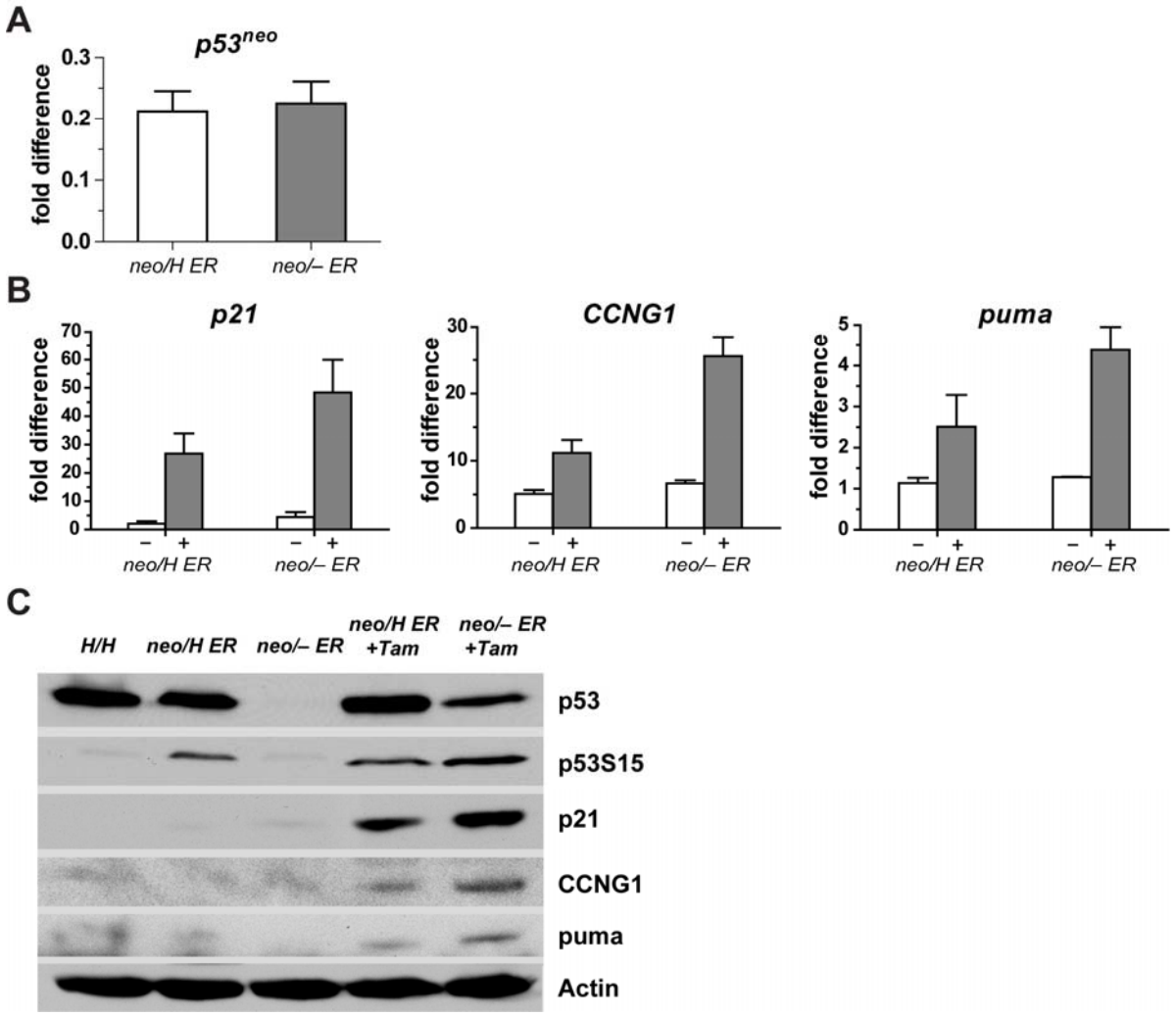

Figure S13. p53R172H Dampened the Transcription Activity of the Restored Wild-Type p53 in MEFs

Early passage 13.5 dpc MEFs were subject to 4-hydroxy-tamoxifen treatment for 2 days followed by doxorubicin treatment for 8 hours. (A) $p53^{neo}$ recombination in $p53^{neo/-}$ *Cre-ER*^{TM} (*neo/– ER*) and $p53^{neo/R172H}$ *Cre-ER*^{TM} (*neo/H ER*) MEFs after 4-hydroxy-tamoxifen treatment. The levels of the $p53^{neo}$ allele remaining in DNA samples of cultured cells were analyzed by quantitative real-time PCR. (B) Comparison of mRNA levels of *p21, cyclin G1* (*CCNG1*), and *puma* in $p53^{neo/-}$ *Cre-ER*^{TM} *(neo/– ER)* and $p53^{neo/R172H}$ *Cre-ER*^{TM} (*neo/H ER*) MEFs with (+) and without (–) 4-hydroxy-tamoxifen (Tam) treatment, using real-time RT-PCR analysis. (C) Western blot analyses of p53, p53Ser15 (p53S15), p21, cyclin G1 (CCNG1), and puma protein levels in MEFs. MEFs of $p53^{R172H/R172H}$ genotype (*H/H*) were used as a control. Expression levels were normalized to actin.

Figure S14

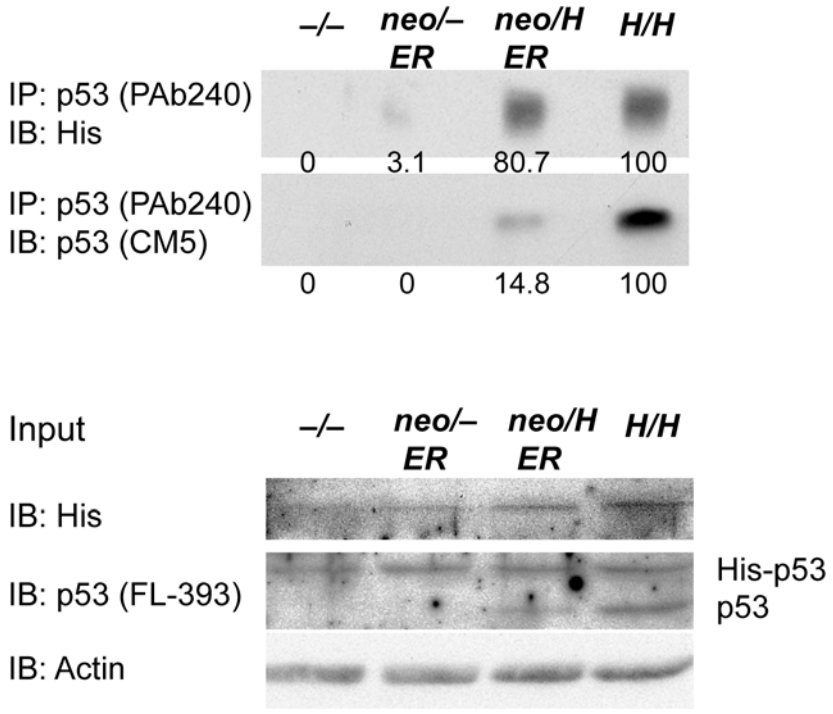

Figure S14. p53R172H Binds to Wild-Type p53 in Sarcoma Tumor Cell Lines

Sarcoma tumor cell lines with genotypes of *p53*$^{-/-}$ (*–/–*), *p53*$^{neo/-}$ *Cre-ER*^{TM} *(neo/– ER), p53*$^{neo/R172H}$ *Cre-ER*^{TM} (*neo/H ER*), and *p53*$^{R172H/R172H}$ (*H/H*) were transfected with pCMV-His-tagged-p53 for 48 hours. Equal amount of cell lysates were immunoprecipitated with p53 PAb240 antibody that recognized mutant p53, then resolved on SDS-PAGE, and immunoblotted with anti-His tag antibody to observe binding of wild-type p53 to mutant p53. The same membrane was also blotted with anti-p53 CM5 antibody to detect mutant p53. The number under each lane indicates the His-tagged-p53 and mutant p53 protein levels (%) relative to H/H (100%). One tenth of the cell lysates (input, lower panel) were examined by immunobloting with His tag antibody to detect transfected His-tagged p53, and with the p53 FL-393 antibody to detect both mutant and wild-type p53. Expression levels of proteins were normalized to actin.